JOURNAL OF APPLIED ELECTROCHEMISTRY 24 (1994) 1102–1108

Fundamental study of the anodic and cathodic reactions during the electrolysis of a lithium carbonate–lithium chloride melt using a carbon anode

W. H. Kruesi*, and D. J. Fray‡

Department of Materials Science and Metallurgy, University of Cambridge, Cambridge CB2 3QZ, Great Britain

Received 18 May 1993; revised 22 January 1994

Cyclic voltammetry, in conjunction with the chromatographic analysis of the anode product, has been used to elucidate the reactions occurring during the electrolysis of lithium carbonate–lithium chloride melts. At a carbonate ion concentration of 0.033 mole fraction the peak anodic current densities were 3100 A m^{-2} on vitreous carbon and 6900 A m^{-2} on graphite with the product being carbon dioxide. The cathodic reduction of carbonate at low concentrations was found to occur at −1.0 V to −1.2 V vs a Ag/Ag(I) reference electrode which is 1.2 V less negative than the potential at which lithium ions were reduced. Voltammetric studies of the reduction of the carbonate ion indicated that the reaction mechanism involved an irreversible charge transfer.

1. Introduction

Lithium is produced by the electrolysis of molten lithium chloride–potassium chloride electrolyte at a temperature of 730–770 K [1–6]. The cells operate at 6–9 V, with current efficiencies of 90%, based on metal recovery which results in an energy requirement of 35–40 kWh kg^{-1} [2, 5, 6]. The production of anhydrous lithium chloride is an energy intensive and expensive process involving the reaction of lithium carbonate with hydrochloric acid and heating the resulting solution above 368 K, where anhydrous lithium chloride crystallizes [7]. The direct feeding of lithium carbonate, which is not hygroscopic, to a cell would remove the energy intensive step and simplify the handling of the feed material. Furthermore, corrosion resistant equipment needed to transport, purify, compress, and store chlorine gas might no longer be needed and this would offer both economic and environmental benefits. Thieler [8], Sintim–Damoa [9] and Kruesi and Fray [10] have shown that it is feasible to feed lithium carbonate to a conventional electrolyte and produce lithium at the cathode and carbon dioxide at the anode.

Chloride and carbonate-chloride mixtures form low melting eutectics [11] and, in solution, the carbonate ion dissociates according to the equilibrium

$$CO_3^{2-}(l) \rightleftharpoons CO_2(g) + O^{2-}(l) \quad (1)$$

Determination of the dissociation constant for lithium carbonate shows that the degree of dissociation is slight below 1000 K [12, 13]. The working potential range of LiCl–KCl eutectic melts, as measured with a Ag/Ag(I) reference electrode, is +1.033 V where chlorine gas is evolved, and −2.543 V where lithium metal deposits [14]. The working potential range of Li_2CO_3–K_2CO_3 melts, as measured with a CO_2, O_2/C reference electrode, is +0.2 V where the anodic reaction

$$CO_3^{2-}(l) = CO_2(g) + \tfrac{1}{2}O_2(g) + 2e^- \quad (2)$$

occurs at an inert electrode to −1.8 to −2.0 V where the reaction

$$CO_3^{2-}(l) + 4e^- = C(s) + 3O^{2-}(l) \quad (3)$$

occurs [14, 15].

Cathodic reduction processes in carbonate melts have been studied by a number of authors because of their importance in molten fuel cell technology [16–20]. This work has shown that alkali metal is deposited from binary melts consisting of sodium and potassium carbonate, however, melts which contained lithium carbonate always resulted in deposition of carbon by Reaction 3. It is, therefore, possible that electrowinning from mixed carbonate–chloride melts may be complicated because carbonate ion reduction will compete with lithium ion reduction.

The electrochemical oxidation of carbon anodes, manufactured from various coals, was investigated in ternary lithium, sodium and potassium carbonate by Weaver and Nanis [21]. The primary anode product was carbon dioxide via the reaction

$$C(s) + 2CO_3^{2-} = 3CO_2(g) + 4e^- \quad (4)$$

Thermodynamically, Reaction 4 is preferred to

$$2Cl^-(l) = Cl_2(g) + 2e^- \quad (5)$$

* Now with Interpro, Golden, CO, USA
‡ Now with the Department of Mining and Mineral Engineering University of Leeds, Leeds LS2 9JT, Great Britain

0021-891X

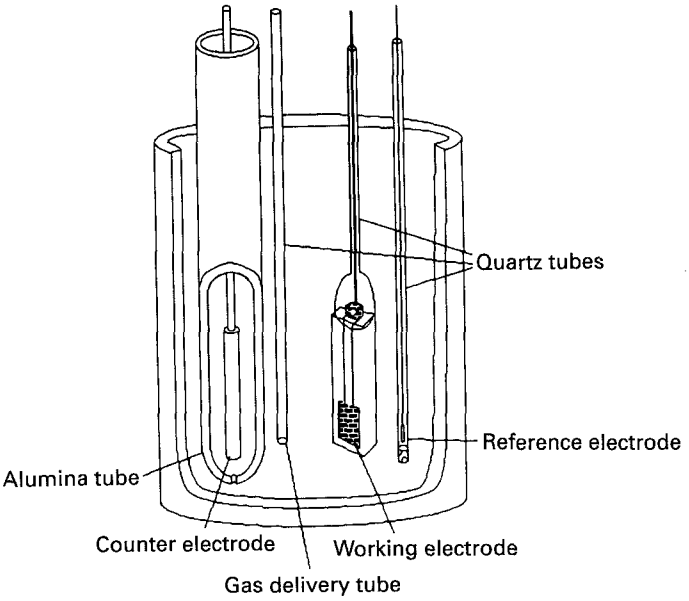

Fig. 1. Diagram showing the arrangement of the electrodes in the CV measurements.

but in mixed carbonate–chloride melts, this needs to be confirmed.

Overall, it should be possible to electrowin lithium from carbonate–chloride melts with CO_2 being evolved at a carbon anode but, as the potentials of the various competing reactions are relatively close, the precise reactions need to be identified.

2. Voltammetric studies of the anode and cathode reactions

The potential–current–time characteristics of a steel electrode, a vitreous carbon electrode, and a graphite electrode in the LiCl–KCl background electrolyte and at various carbonate ion concentrations was studied at 798–803 K using cyclic voltammetry. A Princeton Applied Research (PAR) model 273 potentiostat, interfaced with an Amstrad PC 1640HD20 computer was used to control the cell parameters and to collect the data. The computer directed the potentiostat using EG&Gs Headstart [18] software.

The electrochemical cells were housed in a mullite reaction vessel which held an alumina crucible (7.4 cm i.d., 15 cm height) containing about 240 g of LiCl–KCl eutectic. The working and reference electrodes were suspended in the bulk of the melt, together with a thermocouple, and a quartz tube through which gas was bubbled into the melt. The counter electrode was housed in an alumina tube with a small (0.1 cm diameter) hole in its bottom which allowed flow of current but prevented the mixing of the anodic and cathodic products. Argon (dried through a column of Mg $(ClO_4)_2$) was circulated over the counter electrode. The apparatus is shown schematically in Fig. 1.

Prior to measuring the voltammograms, the LiCl–KCl melt was purified by electrolysis at 0.3 A for 1–2 h using the counter electrode and a removable auxiliary electrode. The lithium carbonate, which was added to the electrolyte, was dried for 2 h in carbon dioxide at 573 K.

2.1. *Cathodic reactions*

Cyclic voltammograms of a mild steel (3.9 cm × 0.65 cm) plate in the electrolyte were measured using a Li–Al (10.8 wt % Li) reference electrode, a Ag/Ag(I) ([AgCl] = 0.4 mole fraction) reference electrode and a graphite counter electrode. The working electrode potential values were swept negatively to −0.6 V vs the Li–Al electrode and −2.6 V vs the Ag/Ag(I) electrode at rates of 50,200 and 400 mV s^{-1}. Voltammograms were collected from the purified electrolyte and at two carbonate ion concentrations after the addition of lithium carbonate.

2.2. *Anodic reactions*

A holder for the vitreous carbon plate was machined out of boron nitride to define the working surface area of the vitreous carbon as 1.06 cm^2. Similarly, an alumina tube was cut to expose an area of graphite rod equal to 0.873 cm^2.

Electrical connections with the vitreous carbon was made by attaching a 0.5 mm platinum wire, using a stainless steel nut and bolt, which was protected from corrosive salt vapours by cementing a quartz bell to the top of the boron nitride holder. Prior to use, the surface of the vitreous carbon was polished to a mirror finish using silicon carbide paper. Electrical connection with the graphite rod was made by threading a mild steel rod into the graphite. Cyclic voltammograms of the vitreous carbon and graphite working electrodes were collected using a Ag/Ag(I) reference electrode and a mild steel counter electrode. The working electrode potential was swept positively through 0.6 V vs Ag/Ag(I) at rates between 10 and 400 mV s^{-1}. Generally, two or three potential sweeps were made before recording a voltammogram in order to condition the electrode surface.

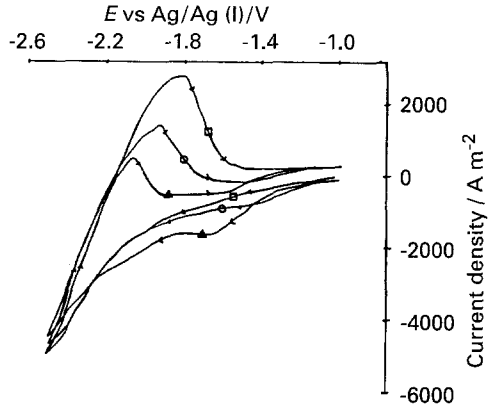

Fig. 2. CVs on a steel electrode in the background electrolyte at mole fractions of carbonate ion of (□) 0, (○) 0.0006 and (△) 0.0018.

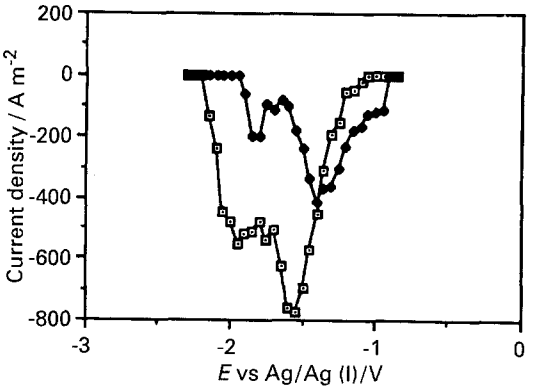

Fig. 3. Resolved current densities of a steel electrode at mole fractions of carbonate ion of (◆) 0.0006 and (⊡) 0.0018.

The voltammograms from the purified LiCl–KCl electrolyte were obtained while dry argon was bubbled through the melt. The argon was replaced by dry carbon dioxide before the addition of lithium carbonate to the melt.

3. Results and discussion

3.1. *Cathodic cyclic voltammetry*

Cyclic voltammetry was used to identify the effect of the carbonate ion concentration on the current density–potential behaviour of the cathode reaction at a steel cathode. Voltammograms were obtained using both a Li–Al reference electrode and a Ag/Ag(I) reference electrode. A potential value of −0.55 V vs Li–Al corresponded to a potential of −2.4 V vs Ag/Ag(I) at 800 K which is in reasonable agreement with previous work [14]. For consistency, all values are reported against the Ag/Ag(I) reference.

Voltammograms for the background electrolyte (LiCl–KCl eutectic) and at two carbonate ion concentrations are shown in Fig. 2. The voltammogram for the background electrolyte shows a sharp rise in current density between −2.2 to −2.6 V vs Ag/Ag(I), which is in good agreement with the published data for the deposition of lithium. The large anodic peak on the reverse scan is due to the dissolution of the lithium deposited during the forward scan. The shape of the lithium deposition curve differs slightly from those found in the literature in that the reverse scan does not cross over the forward scan. This is usually attributed to the overpotential for nucleation in the forward scan and may not have occurred in this work due to sodium deposition, present as an impurity in the electrolyte, at lower potential which can act as a nucleation site for the lithium.

In the presence of carbonate there is an increase in current density at −1.0 to −1.2 V vs Ag/Ag(I). This can be seen more clearly in Fig. 3, where the current densities, due to reduction of the carbonate ion, are resolved by subtracting the background current density from the current density in the presence of the carbonate ion. The results indicate that carbonate ion reduction occurs at much less negative potentials than lithium ion reduction and the peak current density is obviously proportional to the carbonate ion concentration. The less negative potential is contrary to the published similarity in the reduction potentials of lithium ions and carbonate ions in pure carbonates [15].

The reduction reaction is

$$CO_3^{2-}(l) + 4e^- = (e) + 3O^{2-}(e) \qquad (6)$$

and the appropriate Nernst equation is

$$E = E^0 - \left(\frac{RT}{4F}\right) \ln \frac{a_c(a_{O^{2-}})^3}{a_{CO_3^{2-}}} \qquad (7)$$

where E is the potential, E^0 is the potential when all the species are in their standard states, R is the gas constant, T is the temperature, F is Faraday's constant and a is the activity of the given component. The activity of carbon can be taken as unity, $a_{CO_3^{2-}}$ will be less than unity and if the carbonate ion is only slightly dissociated $a_{O^{2-}}$ will be much less than unity making the second term on the RHS of the equation positive, thereby reducing the potential at which cathodic reduction occurs. It can, therefore, be concluded that the carbonate ion undergoes little dissociation in the melt.

It is evident, from the much smaller galvanic current peaks on the reverse scans with carbonate ion present, that either less lithium was deposited due to the reduction of carbonate ion and/or some of the lithium has undergone chemical reaction with the carbonate ion. The lack of a reverse peak associated with the carbonate ion reduction suggests that this is an irreversible reaction with either an irreversible charge transfer or with coupled chemical reactions which limit the reaction rate.

To explore the nature of the reaction mechanism, voltammogams were obtained at three sweep rates with a carbonate ion concentration of 0.0018 mole fraction. The resolved current densities of the forward sweeps are shown in Fig. 4.

The two peaks in Fig. 3 can perhaps be attributed to two separate electron transfer steps in the reduction of the carbonate to carbon reaction. The electron

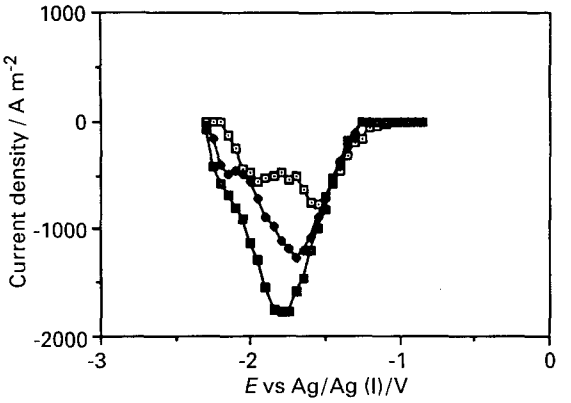

Fig. 4. Resolved current densities on a steel electrode at three potential scan rates with a carbonate ion concentration of 0.0018 mole fraction: (□) 50, (◆) 200 and (■) 400 mV s^{-1}.

transfer of the second (more negative) peak appears to be dependent on the rate of a slow intermediate chemical reaction because as the scan rate is increased the second peak diminishes (Fig. 4). Thus, at faster scan rates, the concentration of reactant in the second reaction is small, leading to a smaller peak. The first reaction is perhaps the reduction of carbonate ion to carbon monoxide or a carbon suboxide which upon further reduction, is converted to carbon.

For an irreversible charge transfer reaction, the equation for the rate of carbonate ion transport (assuming the transport is due entirely to diffusion) is given by Fick's second law:

$$\frac{\delta C_{CO_3^{2-}}}{\delta t} = -D_{CO_3^{2-}}\left(\frac{\delta^2 C_{CO_3^{2-}}}{\delta^2 x}\right) \tag{8}$$

where $C_{CO_3^{2-}}$ is the concentration of the carbonate ion, t is the time, $D_{CO_3^{2-}}$ is the diffusion coefficient of carbonate ion in the melt, and x is the diffusion distance. The solution to Fick's second law with the boundary conditions appropriate for an irreversible charge transfer gives an equation for the current density I of the form [22]

$$I = nFC_{CO_3^{2-}}\left(\frac{\alpha n_a F}{RT} D_{CO_3^{2-}} \nu\right)^{1/2} \chi\left(\frac{\alpha n_a F}{RT}(E_i - E)\right) \tag{9}$$

where n is the charge transferred, F is Faraday's constant, $C_{CO_3^{2-}}$ is the bulk concentration of carbonate ion, α is the transfer coefficient. n_a is the number of electrons transferred up to and including the rate determining step, ν is the potential scan rate, χ represents an integral function which is solvable for particular potential values, E_i is the initial potential of the electrode as measured by the reference electrode and E is the potential at current I. The solution to this equation for the peak current density (i_p) from the tabulated solution [23, 24] of the integral function is

$$i_p = 0.28\pi^{1/2} nFC_{CO_3^{2-}}\left(\frac{\alpha n_a F}{RT} DC_{CO_3^{2-}} \nu\right)^{1/2} \tag{10}$$

From Equation 10 it can be seen that a plot of $i_p \nu^{-1/2}$ against ν gives a very sensitive indication of the relationship of the peak current density to the scan rate. It was found that $i_p \nu^{-1/2}$ is very nearly constant over the range of scans at the carbonate ion concentration of 0.0018 mole fraction, which agrees with the model for an irreversible charge transfer limited reaction. It was also found that the potential at which the peak current density is reached shifts to slightly more negative values with increasing scan rate. This is also consistent with an irreversible charge transfer reaction.

The kinetic parameter, αn_a, can be determined from the shape of the reduced current density curves using the equation [22]

$$E_p - E_{p/2} = -1.857\frac{RT}{\alpha n_a F} \tag{11}$$

where E_p is the peak potential and $E_{p/2}$ is the half peak potential. The values, for the data in Fig. 7, are given in Table 1, together with the calculated values of αn_a.

If n_a, the number of electrons transferred up to and including the rate limiting step, is four then the transfer coefficient (α) is approximately 0.18–0.14. This low transfer coefficient indicates that considerable overvoltage must be applied in order to achieve high current densities due to the reduction of the carbonate ion. However, considering that the reduction of carbonate ions occurs at much less negative potentials than lithium ion reduction in the lithium chloride–potassium chloride melt it is likely that in the electrowinning cell there will be a large cathodic overvoltage relative to carbonate ion reduction. Thus, in dilute solution, the rate of carbonate ion reduction will be limited by the transport of the carbonate ion.

3.2. *Anodic cyclic voltammetry*

Cyclic voltammograms from a planar vitreous carbon electrode with carbonate ion concentrations ranging from 0 to 0.0333 mole fraction were obtained. The voltammograms were made at a sweep rate of 50 mV s^{-1}. The resolved current densities due to the reaction of the carbonate ion with the electrode were obtained by subtracting the current density of the background electrolyte from the current density obtained with carbonate ion present. The resolved current densities are shown in Fig. 5. Similarly, voltammograms and resolved current densities for a section of a graphite

Table 1. Peak and half-peak potentials for the reduction of carbonate ion

E_p/V	$E_{p/2}$/V	ν/mV s^{-1}	αn_a
−1.55	−1.38	50	0.74
−1.70	−1.47	200	0.55
−1.75	−1.52	400	0.56

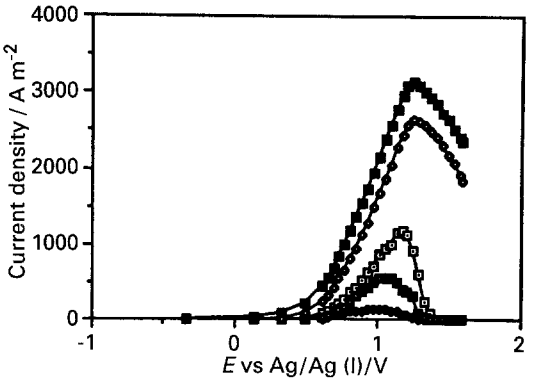

Fig. 5. Resolved current densities on a vitreous carbon electrode at five mole fractions of carbonate ion. Mole fractions: (■) 0.033, (◆) 0.016, (⊡) 0.0041, (■) 0.0023 and (◆) 0.00061.

rod electrode, under the same conditions, are shown in Fig. 6.

The cyclic voltammogram of the background electrolyte (carbonate concentration equal to zero) showed that the potential at which current arises due to the oxidation of chloride ions was +1.17 V vs Ag/Ag(I) on vitreous carbon and 1.08 V on graphite, which is in good agreement with the literature value of +1.033 V [14]. Over the potential range and sweep speed, the current density, due to the oxidation of chloride ions, increased linearly with potential on both vitreous carbon and graphite, indicating that the kinetics of chloride oxidation are fast.

The shape of the reverse sweep of the background electrolyte on the vitreous carbon electrode indicated that the chlorine produced on the forward sweep did not remain on the smooth surface of the electrode because there was no appreciable cathodic current due to chlorine reduction. However, the cathodic peak on the reverse sweep of the background electrolyte on graphite indicated that there was an appreciable amount of chlorine, produced during the forward sweep, which resided on the surface and in the pores of the graphite and was reduced during the reverse sweep giving rise to a cathodic current peak.

As the carbonate ion concentration in the melt was increased a reaction gave rise to a current density, at less positive potentials than the chloride ion oxidation, which was highly dependent on the carbonate ion concentration. The peak current densities are plotted against the carbonate ion concentration for both graphite and vitreous carbon in Fig. 7. It is concluded that up to the peak current density the anode reaction proceeded primarily according to Equation 4 and above the peak current density the anode reaction proceeded as a mixture of the above reaction and Reaction 5.

The extrapolated maximum current densities for the mixed reactions on graphite and vitreous carbon are shown in Fig. 8. For carbonate ion concentrations in the range of 0.016 and 0.033 mole fraction, current densities as high as 14 000 A m^{-2} may be achieved on graphite. The peak current densities obtained on a graphite electrode were much higher than those obtained on a vitreous carbon anode at carbonate ion concentrations of 0.016 mole fraction and above which suggests that the reaction of the carbonate ion with the carbon of the anode is catalyzed on graphite compared to vitreous carbon. However, although there may be some catalytic effect on graphite, the real surface area of the graphite is uncertain and was probably considerably greater than the apparent surface, especially after oxidation.

3.3. *Effects of the scan rate on the anodic reaction*

The effect of the potential scan rate on the current density at vitreous carbon and graphite electrodes was measured to gain insight into the reaction mechanism. Cyclic voltammograms of the vitreous carbon oxide at three scan rates with a carbonate ion concentration of 0.0003 showed that the most positive potential value reached in these scans was below the peak potential value so that, at no time, was the anodic reaction the oxidation of chloride ions.

It is evident from the reverse sweeps, there was no reverse (cathodic) current which suggest that the anode Reaction 4 is irreversible. Considering that

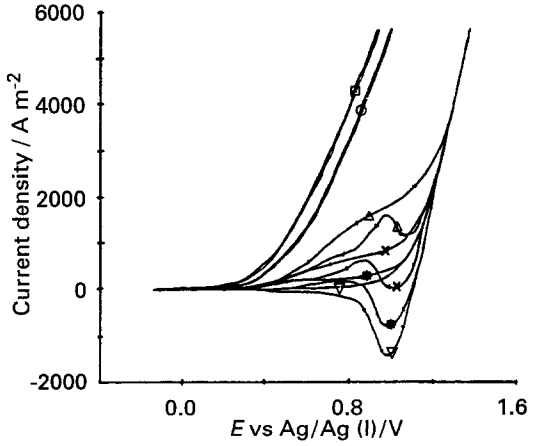

Fig. 6. Cyclic voltammograms on a graphite electrode for the background electrolyte and at five mole fractions of carbonate ion. Mole fractions: (□) 0.033, (○) 0.016, (△) 0.0041, (×) 0.0023, (*) 0.00061 and (▽) 0.

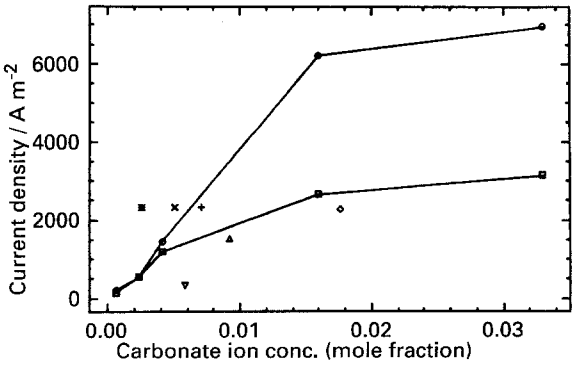

Fig. 7. Relation of the peak current density on graphite and vitreous carbon electrodes to the carbonate ion concentrations. (□) V.C. (○) graphite, (+) cell 2–1, (×) cell 2–2, (■) cell 2–3, (△) cell 5–1, (◇) cell 6–3 and (▽) cell 7–3.

Table 2. Peak current densities and corresponding potentials for vitreous carbon

$[CP_3^{2-}]$/mole fraction	E_p/V	i_p/A m^{-2}	ν/mV s^{-1}	$i_p\nu^{-1/2}$/A m^{-2} mV$^{-1/2}$ s$^{-1/2}$
0.00061	0.972	141.5	50	20.0
0.00061	1.012	254.7	200	18.0
0.00061	1.053	367.9	400	18.4
0.0023	1.092	547.1	50	77.4
0.0041	1.172	1179	50	167
0.0041	1.172	1302	200	92.1
0.0041	1.172	1396	400	69.8
0.016	1.252	2651	50	375
0.033	1.252	3141	50	444
0.033	1.252	3311	200	234
0.033	1.252	3405	400	170

Reaction 4 involves a multiple electron transfer, the dissociation of the carbonate ion, either in the bulk of the melt or at the electrode surface, and the reaction with the anode material resulting in its consumption it is likely that the overall reaction consists of a large number of steps any one of which may be rate determining.

The peak current densities and the corresponding potentials for vitreous carbon are shown in Table 2. Using Equation 10 it was found that the relation of the peak current density to the square root of the scan rate at low carbonate concentrations (0.0061 mole fraction) was very nearly constant over the scan rate range for both vitreous carbon and graphite. This is in excellent agreement with the results of Seon *et al.* [25] who concluded that because of the agreement of the data with that predicted for irreversible electron transfer the dissociation of the carbonate ion does not limit the reaction rate, and Reaction 4 was an irreversible electron transfer reaction. This mechanism also agrees with the near linear increase of peak current density with carbonate ion concentration at low carbonate ion concentration.

Values of αn_a, derived from the application of Equation 11 to the data at the carbonate ion concentration of 0.00061 mole fraction on vitreous carbon and graphite are presented in Table 3.

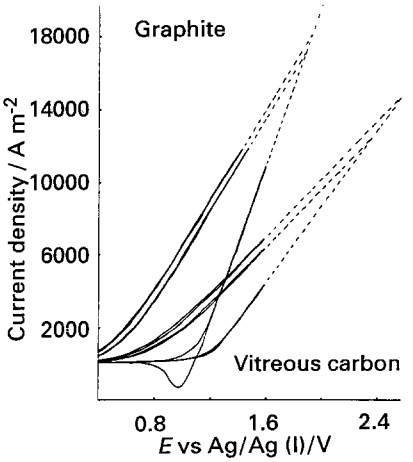

Fig. 8. CVs on vitreous carbon and graphite electrodes for the background electrolyte at two carbonate ion concentrations (0.016 and 0.033 mole fractions) show up the extrapolated highest current densities for the mixed reactions.

If n_a is two, the transfer coefficient is 0.28–0.24, which is in very good agreement with the value of 0.27 found by Seon and coworkers [25]. Again, similar to the reduction of carbonate ion, the transfer coefficient for reaction is relatively low indicating that large overvoltages must be applied to achieve high current densities.

At high carbonate ion concentrations, $i_p\nu^{-1/2}$ decreased with increasing scan rate which may be due to the fact that as the carbonate ion concentration increases it begins to carry a higher proportion of the ionic current and the effects of migration of the carbonate ion may influence the current density. Another possibility is that at higher carbonate ion concentrations the rate of the chemical reaction step in the overall reaction becomes rate determining. At low carbonate ion concentration and low current densities, the anode surface may not be saturated with surface oxides, whereas at high carbonate ion concentration and high current densities the surface may be saturated with surface oxides and the chemical reaction involving the desorption of carbon dioxide may limit the overall reaction rate.

It is interesting to compare these observations with those made from studies of the anode reaction in aluminium smelting. Various authors [26–28] have proposed that the anode current is limited by a chemical reaction: most likely the desorption of the oxide species. However, Welch and coworkers [29] proposed that the electron transfer step is rate determining. For irreversible electrode processes, limited by electron transfer or by a chemical reaction, the current-potential behaviour is very similar.

Table 3. Kinetic parameters for the anodic reaction of carbonate ion (0.000 61 mole fraction) with vitreous carbon and graphite

Vitreous carbon			*Graphite*		
*$E_{p/2}$/V	ν/mv s^{-1}	αn_α	$E_{p/2}$/V	ν/mV s^{-1}	αn_a
0.752	50	0.582	0.353	50	0.494
0.762	200	0.520	0.501	200	0.554
0.784	400	0.480	0.507	400	0.483

* $E_{p/2}$ is the half-peak potential

4. Conclusions

The cathodic reduction of carbonate ions at low concentrations was found to occur at −1.0 V to −1.2 V vs Ag/Ag(I) which is 1.2 V less negative than the potential at which lithium ions reduced. Voltammetric studies of the reduction of carbonate ion indicated that the reaction mechanism involves an irreversible charge transfer. The large cathodic overvoltage, relative to the carbonate ion reduction, that will be present in a lithium electrowinning cell means that, for efficient electrowinning, the supply of carbonate ions to the cathode must be restricted.

It was found that the carbonate ion in a LiCl–KCl eutectic melt reacts with the carbon anode at less positive potentials than chloride ion oxidation.

Cyclic voltammetry studies of the anodic reaction identified the maximum or peak current densities due to the reaction of carbonate ion with vitreous carbon and graphite anodes. With a carbonate ion concentration of 0.033 mole fraction the steady state peak current densities were 3100 $A\,m^{-2}$ on vitreous carbon and 6900 $A\,m^{-2}$ on graphite. The increase in the peak current density with increasing carbonate ion concentrations was largest and nearly linear in the range of 0.000 61 to 0.016 mole fraction.

At carbonate ion concentrations greater than 0.016 mole fraction, the peak current density increased at a much slower rate with increasing carbonate ion concentration.

The dependence of the current density due to the reaction of the carbonate ion with vitreous carbon and graphite on the potential scan rate was consistent with an irreversible charge transfer controlled mechanism at a carbonate ion concentration of 0.000 61 mole fraction. A transfer coefficient of 0.29–0.24 was calculated assuming the number of electrons transferred up to and including the rate determining step was two. The low transfer coefficient indicates the reaction requires large overvoltages in order to achieve high current densities. At higher carbonate ion concentrations the current density–potential scan rate behaviour was consistent with a reaction controlled mechanism.

Acknowledgement

The authors are grateful to London and Scandinavian Metallurgical Co. Ltd for their financial support.

References

[1] W. A. Averill and D. L. Olson, *Energy* **3** (1978) 305.
[2] P. Mahi, A. A. J. Smeets, D. J. Fray and J. A. Charles, *J. Metals* **38** (1986) 20.
[3] W. E. Cowley, 'The Alkali Metals', *in* 'Molten Salt Technology', (edited by D. G. Lovering), Plenum Press, New York (1982) pp. 57–87.
[4] P. E. Landolt, 'Lithium', *in* 'Rare Metals Handbook'. (edited by C. A. Hampel) Reinhold, New York (1954) pp. 215–43.
[5] C. L. Mantell, 'Electrochemical Engineering', McGraw-Hill, New York (1960).
[6] G. T. Motock, *Electrochem. Tech.* **1** (1963) 122.
[7] R. O. Bach, R. B. Ellestad, C. W. Kamienski and J. R. Wassson, 'Lithium and Lithium Compounds;, *in* 'Kirk–Othmer: Encyclopedia of Chemical Technology', Vol. 14. 3rd edition, John Wiley & Sons, New York (1981) pp. 448–76.
[8] E. Thieler, E. 'Method of Producing Lithium', *US Patent 3 344 049* (1967).
[9] K. Sintim-Damoa, S. Srinivasa, N. Reddy and S. McCormack, 'Electrolytic Production of Lithium Metal', *US Patent 4 455 202* (1984).
[10] W. H. Kruesi and D. J. Fray, submitted to *Trans. Met. Soc. B* for publication.
[11] E. M. Levin, C. R. Robbins and H. F. McMurdie, 'Phase Diagrams for Ceramists', The American Ceramists Society, Columbus, OH, USA (1964).
[12] R. Combes, R. Feys and B. Tremillon, *J. Electronanal. Chem.* **83** (1977) 383.
[13] G. Picard, F. Seon and B. Tremillon, *ibid.* **102** (1979) 65.
[14] N. Q. Minh and L. Redey, 'Reference Electrodes for Molten Electrolytes', *in* 'Molten Salt Techniques', Vol. 3, (edited by D. G. Lovering and R. J. Gale), Plenum Press, New York, (1987).
[15] J. R. Selman and H. C. Maru, 'Physical Chemistry and Electrochemistry of Alkali Carbonate Melts', *in* 'Advances in Molten Salt Chemistry', Vol. 4, (edited by G. Mamantov and J. Braustein), Plenum Press, New York (1981), pp. 159–389.
[16] J. Dubois, J. Millet and S. Paulous, *Electrochim Acta,* **12** (1967) 241.
[17] M. D. Ingram, B. Baron and G. J. Janz, *ibid.* **11** (1966) 1629.
[18] H. E. Bartlett and K. E. Johnson, *J. Electrochem. Soc.* **114** (1967) 457.
[19] P. Drossbach and D. Sauermann, *Electrochimica Acta* **9** (1964) 1373.
[20] P. K. Lorenz and G. J. Janz, *ibid.* **9** (1964) 1373.
[21] R. D. Weaver and L. Nanis, 'Electrochemical Oxidation of Carbon in a Molten Carbonate Cool-Air Fuel Cell', *in* Proceedings of the 3rd International Symposium on Molten Salts, (edited by G. Mamantov, M. Blander and G. P. Smith), The Electrochem. Society, Pennington, NJ (1981) pp. 316–33.
[22] A. J. Bard and L. R. Faulkner, 'Electrochemical Methods', John Wiley & Sons, New York (1980).
[23] L. Nadjo and J. M. Saveant, *J. Electroanal. Chem.* **48** (1973) 113.
[24] R. S. Nicholson and J. Shain, *Analytical Chem.* **36** (1964) 706.
[25] F. Seon, G. Picaro and B. Tremillon, *Electrochimica Acta* **27** (1982) 1367.
[26] J. Thonstad, *J. Electrochem. Soc.* **3** (1964) 955.
[27] J. Thonstad, *Electrochimica Acta* **15** (1970) 1581.
[28] H. Stern and G. T. Holmes, *J. Electrochem. Soc.* **105** (1958) 478.
[29] B. I. Welch and N. E. Richards, 'Anodic Overpotentials in the Electrolysis of Alumina, *in* 'Extractive Metallurgy of Aluminium', Vol. 2, Interscience Publishers, John Wiley & Sons, New York (1963) pp. 15–30.